

**IN SILICO ANALYSIS OF RPO B PROTEIN WITH ACTINOMYCIN D
COMPOUND ISOLATED FROM *STREPTOMYCES PARVULUS* SDMRI 3 - NOVEL
STRAIN IDENTIFIED FROM PUNNAKAYAL MANGROVE**

V. Bharathi^{1*}, P. Jamila², Sureshkumar B.T², Srinivasan P³ and Rajalakshmi M³

¹Department of Microbiology, Vivekanandha Arts and Science College for Women,
Veerachipalayam, Sankari West (PO), Sankari, Salem - 637303, Tamilnadu, India.

²Suganthi Devadason Marine Research Institute, Tuticorin-628001, Tamilnadu, India.

³Department of Microbiology, Rathinam College of Arts and Science, Rathinam Tech Zone,
Pollachi Road, Eachanari, Coimbatore -641021, Tamilnadu.

Corresponding Author - bharathi79micro@gmail.com

ABSTRACT

The present study was conducted to identify the binding interaction between the rho B protein with Actinomycin D compound isolated from *Streptomyces parvulus* SDMRI – 3 isolated from Punnakayal mangrove ecosystem of tuticoirn found to be an efficient producer of bioactive compound. The most identical sequences were determined by BLASTP analysis of target sequences of the DNA dependent RNA polymerase from *Bacillus cereus*, *Escherichia coli*, *Enterobacter aerogenes*, *Klebsiella pneumoniae*, *Pseudomonas aeruginosa*, and *Staphylococcus aureus* against the PDB database. Docking interactions indicated that Actinomycin D has a significant interaction with *Staphylococcus aureus* rho B. In *Pseudomonas aeruginosa*, has less docking score. The docking score varies between -7.1652 to -9.2351 kJ/mol. The docking interactions proposed that Actinomycin D isolated compound from novel actinomycetes strain *Streptomyces parvulus* SDMRI -3 has good interaction with rho B protein of *Bacillus cereus*, *Escherichia coli*, *Enterobacter*, and *Klebsiella pneumoniae* via two bonded interactions and four non-bonded interactions, the current study found that the sediments of the Punnakayal mangrove habitat contain potential antibiotic generating bioactive Actinomycetes. *Streptomyces parvulus* SDMRI - 3 was found as a novel Actinomycete strain and registered in the GenBank with this Accession No. KF818457. Actinomycin D is chemical compound isolated from the novel strain having strong interactions with rho B protein from *Staphylococcus aureus*. This isolate is a natural source of the medicinal chemical actinomycin D, which is useful in the development of innovative medications for humans.

Keywords: Homology modeling, Actinomycin D, *Streptomyces Parvulus*, rpo B protein, Docking

1. INTRODUCTION

There is an increase in morbidity and death brought on by infectious microorganisms as a result of the failure of conventional therapies caused by the introduction and spread of antibiotic resistance [1]. So, combating bacterial infections is challenging. A prominent member of the actinomycin family of chromo peptide antibiotics, Actinomycin D (dactinomycin) has a common phenoxazine chromophore connected to two pentapeptide lactone moieties [2]. The number of amino acids in these antibiotics varies. One of this pharmacological. *Streptomyces* synthesizes them as mixes of several actinomycins. However, the *S. parvulus* species mostly (>95%) manufactures actinomycin D [3]. Actinomycin D, Manumacin A, B, and C,

Borrelidin as well as Oleficin, were all known to be synthesized by the *S. parvulus* strain 2297, which Waksman first identified in 1940 [4]. Since Act-D can crosslink inside duplex DNA, hinder DNA-dependent RNA polymerase, and thwart protein synthesis, it has become a crucial tool in medical, developmental, and molecular [5]. We used Actinomycin D, which interferes with DNA to prevent transcription [6]. Actinomycin D (ActD), a commonly used, established biochemical approach, inhibits gene transcription. When used properly, it can be a potent tool for determining messenger RNA (mRNA) degradation rates [7]. It's a common transcription inhibitor. Act D is particularly toxic to RNA polymerase I, which catalyzes ribosomal RNA transcription (IC₅₀, 0.05 g/mL), while RNAP II (0.5 g/mL) and RNAP III (approximately 5 g/mL) are less sensitive [8].

Actinomycin D has been shown to prevent anaerobic glycolysis and respiration in human leukemic leukocytes [9], and transfer of amino acids in bacteria [10]. Actinomycin D caused cellular P53-independent apoptosis, which had cytotoxic and anticancer effects [11]. Actinomycin D was also shown to improve the therapeutic effectiveness of a few anticancer medications that are being used in clinical studies or clinics. It revealed cooperative cytotoxicity with the immunotoxin RG7787 [12]. Specifically, this study uses molecular docking to determine how actinomycin D interacts with the rpo B protein, which is a component of DNA-dependent RNA polymerase.

2. MATERIALS AND METHODS

2.1. Target sequence and potential template search

The KEGG (<http://www.genome.ad.jp/kegg/kegg2.html>) Kyoto Encyclopaedia of Gene and Genomes was searched for the DNA-dependent RNA polymerase, rpo B protein sequences of *Bacillus cereus*, *Escherichia coli*, *Enterobacter*, *Klebsiella pneumoniae*, *Pseudomonas aeruginosa*, and *Staphylococcus aureus*. Template sequences were obtained via the NCBI-Blast search on the Protein Data Bank (PDB) in order to build a three-dimensional structure [13]. The sequence that was found to be the most homologous was taken into account as a potential template structure for homology modelling. The atomic coordinate file for the template structure was retrieved from the PDB [14].

2.2. Homology modelling of rpo B protein

SWISS-MODEL is a homology-modeling server that utilizes the structures available from the [ExPASy](http://swissmodel.expasy.org) web server (<http://swissmodel.expasy.org>) or the program DeepView (Swiss PDB - Viewer) In order to create the model, the ultimate sequence alignment file of the target and template sequences as well as the atomic coordinates files of the template structure were used. The server offers completely automated model creation, alignment, and design collecting. The server can produce a model in a few minutes or over several hours due to the intricacy of the modeling and database [15]. A particular bundle of models from the created 3D models was chosen and used in the calculation.

2.3. Model assessment

PROCHECK, Verfiy3D, and ERRAT of the SAVES server further verified the created models for their overall stereochemical properties. The best models were chosen for docking experiments based on the Ramachandran plot because they showed an increased percentage of residues in the most favourable regions and fewer residues in the disallowed regions [16].

2.4. Prediction of binding site

With Q-site Finder or Active site prediction server, the active sites of the simulated rho B protein are identified. To ascertain the binding affinity between simulated rho B and actinomycin D, molecular docking is then carried out [17].

2.5. Ligand generation and flexible docking

ACD-Chemsketch was used to create the Actinomycin D 2D structure and generate its SMILES notation. 'Online SMILES convertor and Structure file generator' was used to convert the retrieved 2D SDF file formats into common 3D PDB formats for additional *in silico* studies [18]. Using FlexX, [19], the generated SDF structures were docked with the amino acids in the binding site of rpo B protein from *Bacillus cereus*, *Escherichia coli*, *Enterobacter*, *Klebsiella pneumoniae*, *Pseudomonas aeruginosa*, and *Staphylococcus aureus* with the parameters listed

- i) Typical general docking information,
- ii) triangle matching for base placement, full score contribution and a threshold of 0,30, and no scoring contribution and a cutoff of 0,70.
- iii) Chemical parameters of conflict handling values for protein-ligand interactions with the maximum permitted overlap volume of 2.9 \AA^3 and intra-ligand interactions with a clash factor of 0.6 and taking hydrogen into account in internal clash testing.
- iv) By default, both the maximum number of solutions per iteration and the maximum number of solutions per fragmentation is set to 200.

2.6. Prediction of ligand-receptor interactions

The pose-view of LeadIT was used to analyse the interactions between the Actinomycin D molecule and the amino acids in the binding site of rho B from *Bacillus cereus*, *Escherichia coli*, *Enterobacter*, *Klebsiella pneumoniae*, *Pseudomonas aeruginosa*, and *Staphylococcus aureus* in the docked complex [20].

3. RESULTS

3.1. Sequence analysis and potential template for homology modelling

The PDB database was used in the BLASTP analysis of the target sequences of the DNA-dependent RNA polymerase from *Bacillus cereus*, *Escherichia coli*, *Enterobacter*, *Klebsiella pneumoniae*, *Pseudomonas aeruginosa*, and *Staphylococcus aureus*. The results showed that crystal structures were the most homologous sequences. The PDBID, sequence identity, and E-value of the respective rpo B were shown in Table 1.

Table 1: Modelled structure and its template details

Organism	Target	Template	Similarity	E value
<i>Bacillus cereus</i>	DNA-directed RNA polymerase (rpoB)	4ljz (Chain)	66.46%	4.12e-56
<i>Staphylococcus aureus</i>	DNA-directed RNA polymerase (rpoB)	3tbi (B_chain)	70.09%	1.92e-34
<i>Escherichia coli</i>	DNA-directed RNA polymerase (rpoB)	4kn4 (C_chain)	100%	0.00
<i>Pseudomonas aeruginosa</i>	DNA-directed RNA polymerase (rpoB)	3iyd(C_chain)	79.01%	0.00

<i>Enterobacter aerogenes</i>	DNA-directed RNA polymerase (rpoB)	3iyd(C_chain)	99.54%	0.00e-1
<i>Klebsiella pneumoniae</i>	DNA-directed RNA polymerase (rpoB)	3iyd(C_chain)	98.88%	0.00e-1

3.2. Homology modeling of rpoB

The initial model of rpoB was created using SwissModel Server utilizing the sequences from *Bacillus cereus*, *Escherichia coli*, *Enterobacter*, *Klebsiella pneumoniae*, *Pseudomonas aeruginosa*, and *Staphylococcus aureus* as input. A collection of models were created using random generation. The modelled structures of rpoB from *Staphylococcus aureus*, *Escherichia coli*, *Bacillus cereus*, *Enterobacter*, *Klebsiella pneumoniae*, and *Pseudomonas aeruginosa* are depicted in Figure 1(A-F).

3.3. Model Assessment

The entire stereochemical parameters were evaluated by PROCHECK, Verify3D, and ERRAT of the SAVES server to determine the accuracy of the created models. Over 80% of the residues in the most favourable regions were visible in the Ramachandran plot of all rpoB models that had been developed (Figure 2A-F). Table 2 shows the percentage of residues in each rpoB from *Bacillus cereus*, *Escherichia coli*, *Enterobacter*, *Klebsiella pneumoniae*, *Pseudomonas aeruginosa*, and *Staphylococcus aureus* that are in the most favourable regions, additionally allowed regions, generously allowed regions, and disallowed regions. Additionally, ERRAT and Verify 3D were used to observe and tabulate the overall quality factor and the compatibility of an atomic model (3D) with the amino acid sequence (1D) for the modelled proteins rpoB. The model's reliability and preciseness were further supported by the outcomes of ERRAT and Verify-3D.

Table 2: Modelled structure validation details at the SAVES server

Organism	Protein	Residues and their percentage in Ramachandran plot (PROCHECK)				Verify 3D	ERRAT
		MFR	AAR	GAR	DAR		
<i>Bacillus cereus</i>	DNA-directed RNA polymerase (rpoB)	85.2%	14.1%	0.0%	0.7%	84.99%	79.667
<i>Staphylococcus aureus</i>	DNA-directed RNA polymerase (rpoB)	89.0%	11.0%	0.0%	0.0%	92.63%	98.734
<i>Escherichia coli</i>	DNA-directed RNA polymerase (rpoB)	85.9%	12.2%	1.1%	1.1%	94.88%	98.227
<i>Pseudomonas aeruginosa</i>	DNA-directed RNA polymerase (rpoB)	84.0%	13.6%	1.2%	1.2%	100%	97.518

<i>Enterobacter aerogenes</i>	DNA-directed RNA polymerase (rpoB)	86.6%	11.5%	0.8%	1.1%	100%	98.582
<i>Klebsiella pneumonia</i>	DNA-directed RNA polymerase (rpoB)	86.6%	12.3%	0.0%	1.1%	95.24%	84.211

3.4. Binding Site Prediction

The ten potential binding sites for the DNA-dependent RNA polymerase rpoB from *Bacillus cereus*, *Escherichia coli*, *Enterobacter*, *Klebsiella pneumoniae*, *Pseudomonas aeruginosa*, and *Staphylococcus aureus* are shown in Figure 3 (A-F). The initial predicted binding site (blue color) is thought to be the best binding location and is utilized for additional docking experiments.

3.5. Docking studies

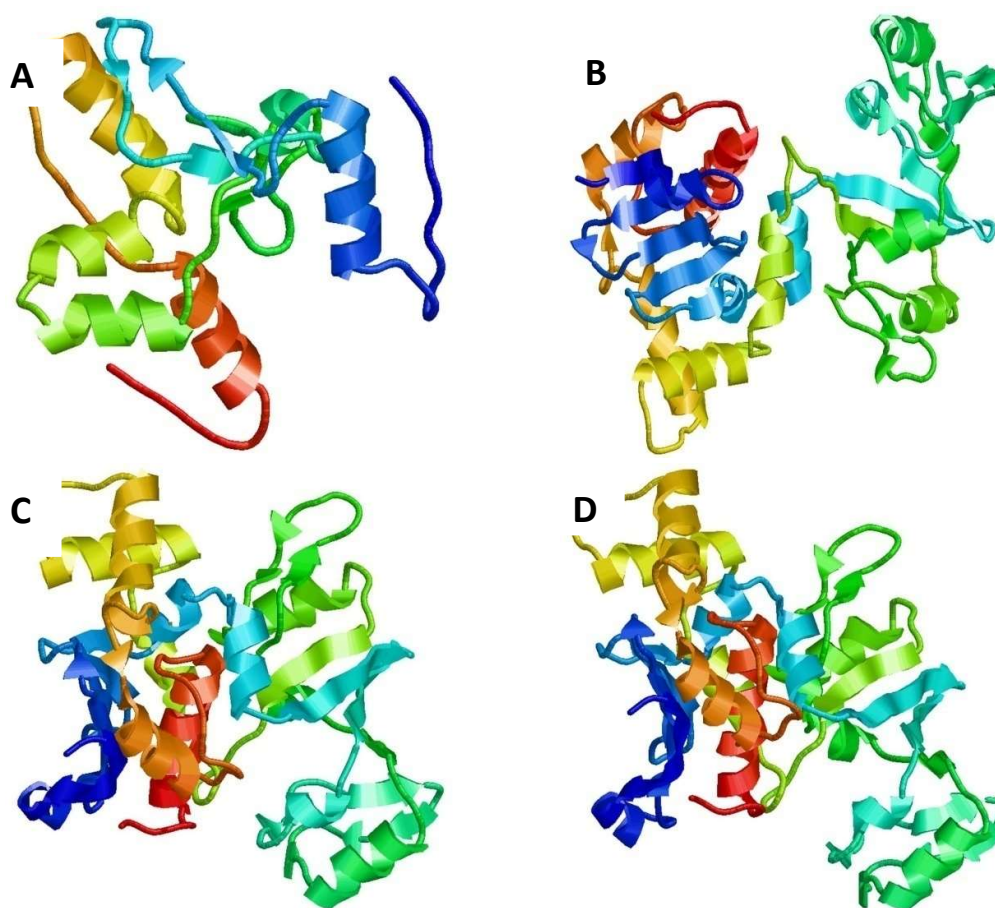
DNA-dependent RNA Polymerase rpoB from *Bacillus cereus*, *Escherichia coli*, *Enterobacter*, *Klebsiella pneumoniae*, *Pseudomonas aeruginosa*, and *Staphylococcus aureus* docked with the Actinomycin D molecule are shown in Figure 4 (A-F). Table 3 displays the docking interactions and associated binding scores between the Actinomycin D and rpoB binding site residues.

Table 3: Docking interactions residues of DNA-dependent RNA Polymerase rpoB with Actinomycin D and their docking score

Sr. no.	Organism	Protein	Bonded	Non bonded	Docking score (kJ/mol)
1	<i>Bacillus cereus</i>	rpoB	Lys1098 Gln1072	Gly1071 Arg1050 Lys1098 Ser1051	-8.2345
2	<i>Staphylococcus aureus</i>	rpoB	Gly344 Phe224	Ile433 Asp342 His343 Asp434	-7.5362
3	<i>Escherichia coli</i>	rpoB	Glu226 Gly344	Phe225 Asp342 Ile433 His343	-8.1465
4	<i>Pseudomonas aeruginosa</i>	rpoB	Glu237 Gly355	Phe236 Asp353 Ile444 His354	-8.2187
5	<i>Enterobacter aerogenes</i>	rpoB	Phe351 Phe228	Gly349 Phe351 Val438	-7.1652

				Asp347 Asp439	
6	<i>Klebsiella pneumoniae</i>	rpoB	Leu887 His790	Ile885 Ile791 Leu887 His790 Val886 Gly884 Val835 Tyr794	-9.2351

Figure 1 Modelled structure of DNA-dependent RNA polymerase (rpoB). a. rpoB from *Bacillus cerus*; b. rpoB from *Escherichia coli*; c. rpoB from *Enterobacter*; d. rpoB from *Klebsiella pneumonia*; e. rpoB from *Pseudomonas aeruginosa*; f. rpoB from *Staphylococcus aureus*



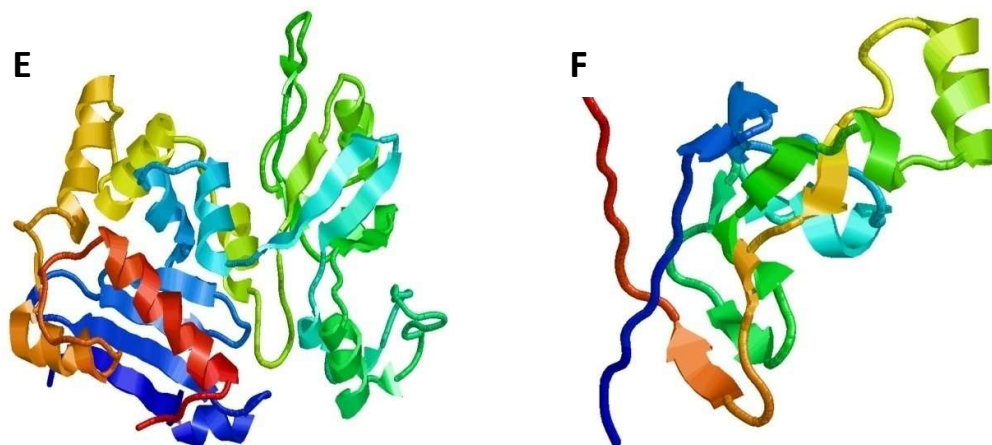
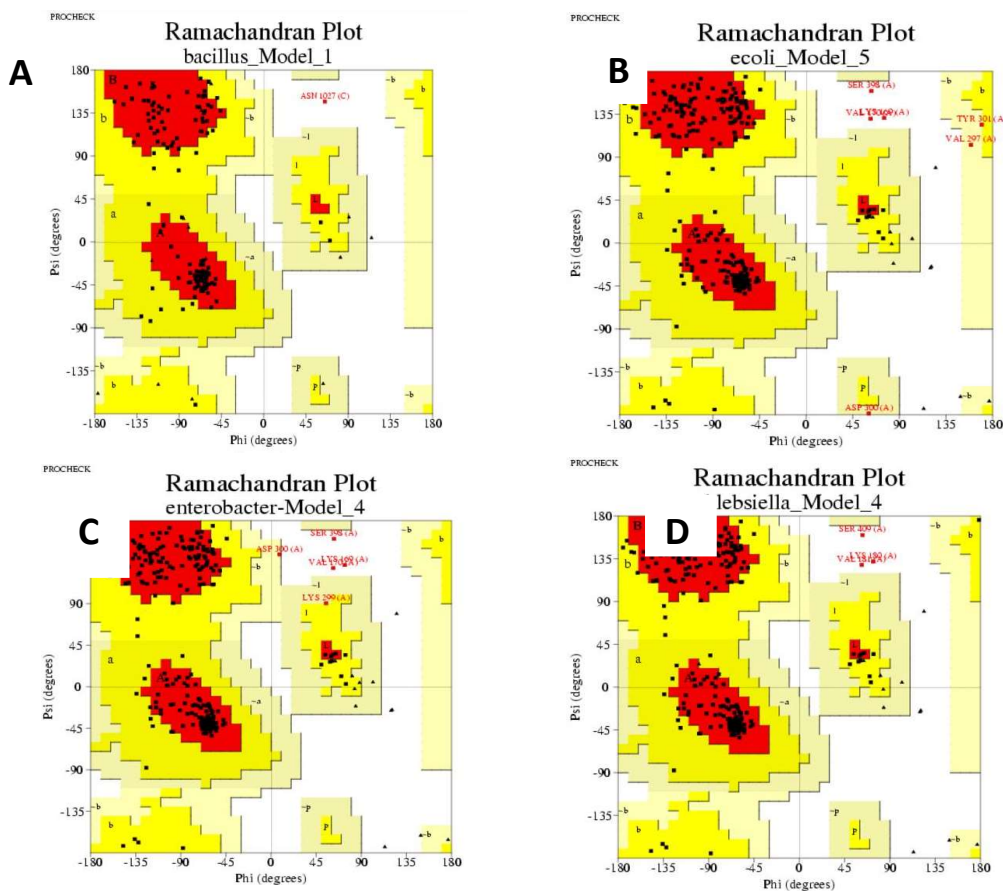


Figure.2. Ramachandra plot for the Modeled structure of DNA-dependent RNA polymerase (rpoB) using Procheck at SAVES Server. A. rpoB from *Bacillus cereus*; B. rpoB from *Escherichia coli*; C. rpoB from *Enterobacter*; D. rpoB from *Klebsiella pneumoniae*; E. rpoB from *Pseudomonas aeruginosa*; F. rpoB from *Staphylococcus aureus*



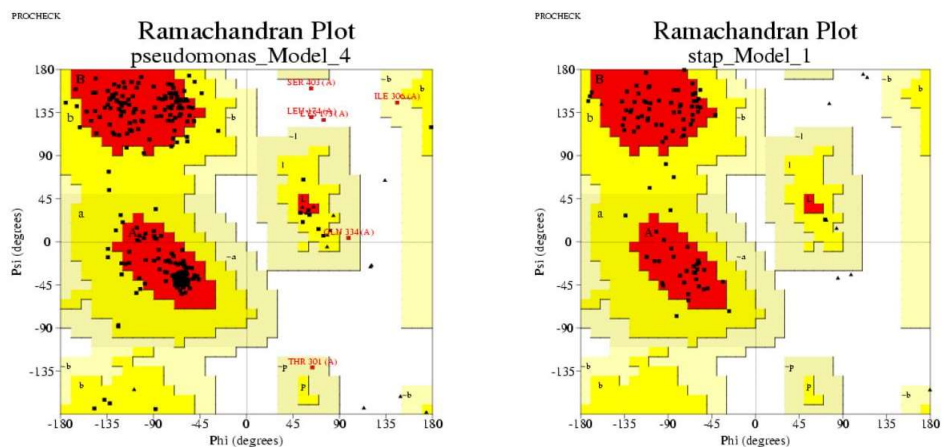
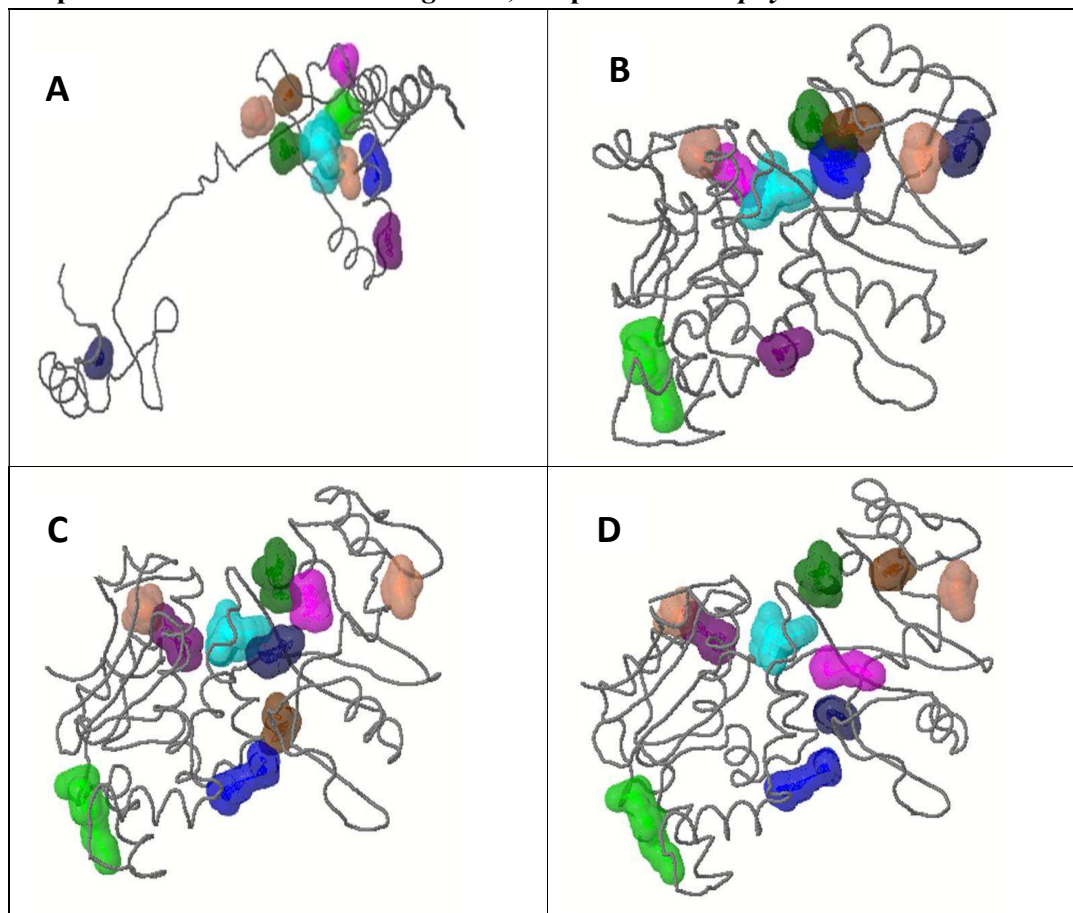


Figure.3. Ten predicted binding sites of the Modeled structure of DNA-dependent RNA polymerase (rpoB) using Q-site Finder server. A. rpoB from *Bacillus cereus*; B. rpoB from *Escherichia coli*; C. rpoB from *Enterobacter*; D. rpoB from *Klebsiella pneumonia*; E. rpoB from *Pseudomonas aeruginosa*; F. rpoB from *Staphylococcus aureus*.



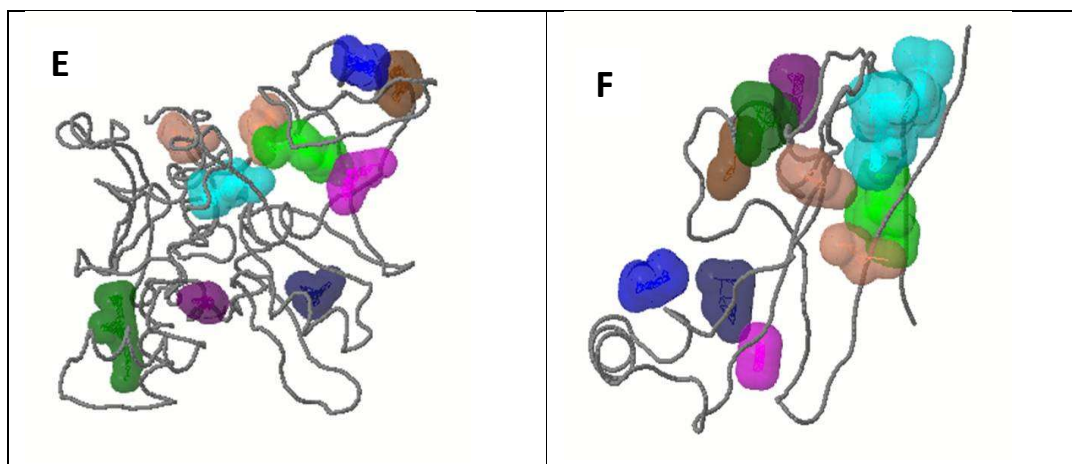
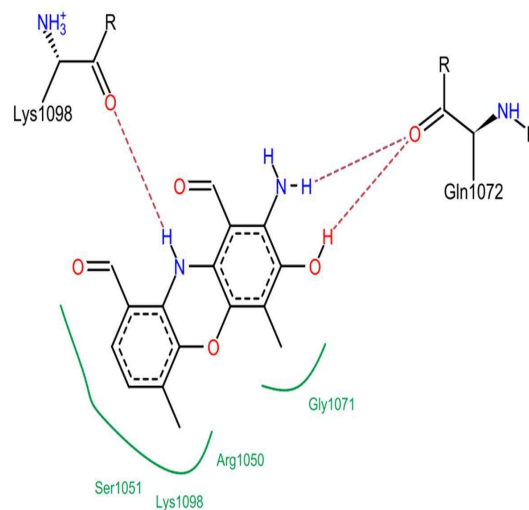
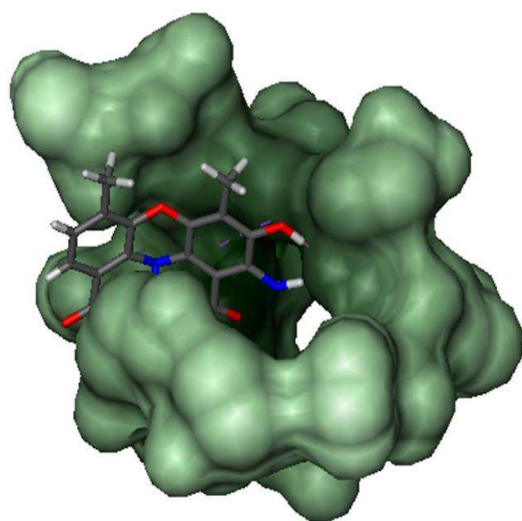


Figure 4. a. Docking complex and its interactions of rpoB from *Bacillus cereus* and Actinomycin D. . b. Docking complex and its interactions of rpoB from *Escherichia coli* and Actinomycin D

a.



b.

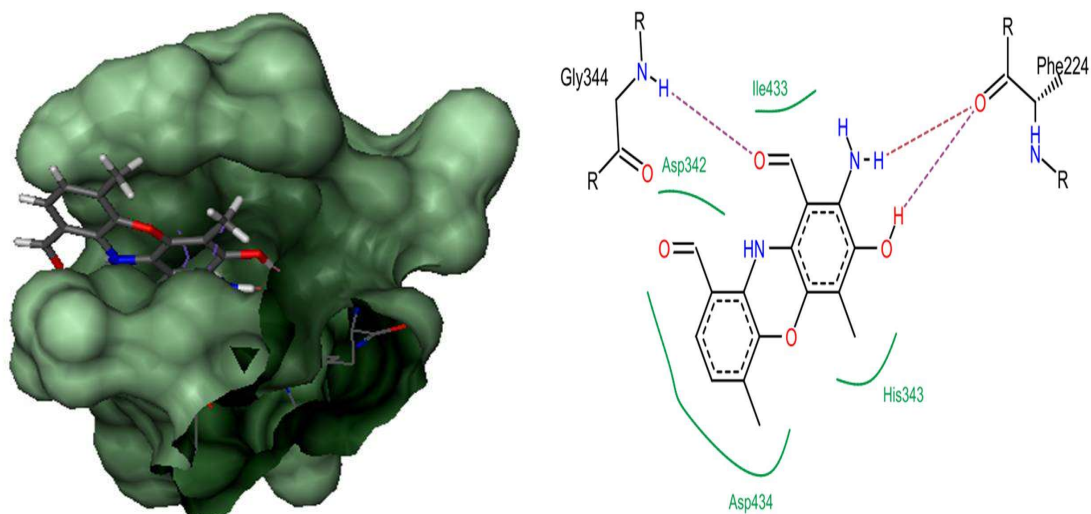
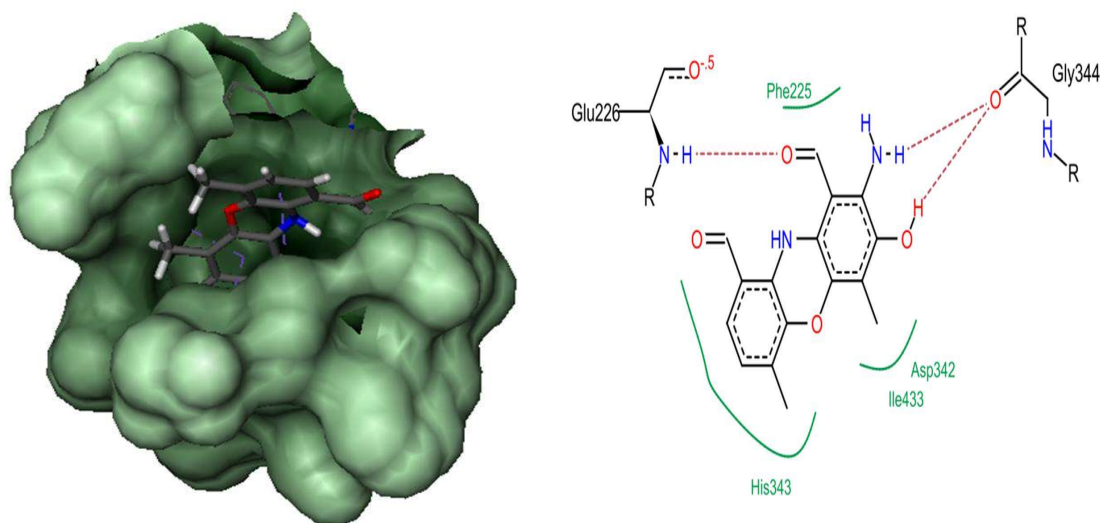


Figure 4. c. Docking complex and its interactions of rpoB from *Enterobacter* and Actinomycin D. d. Docking complex and its interactions of rpoB from *Klebsiella pneumonia* and Actinomycin D



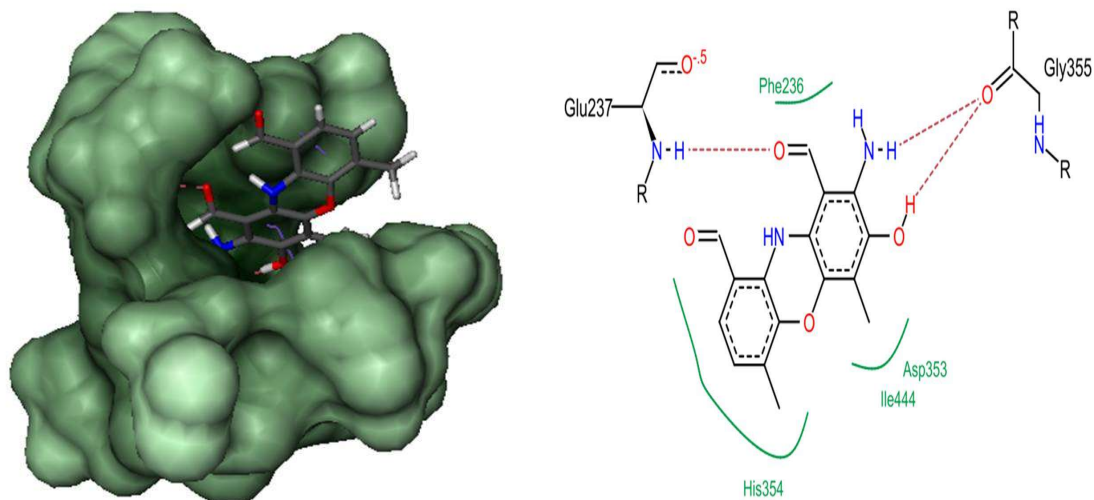
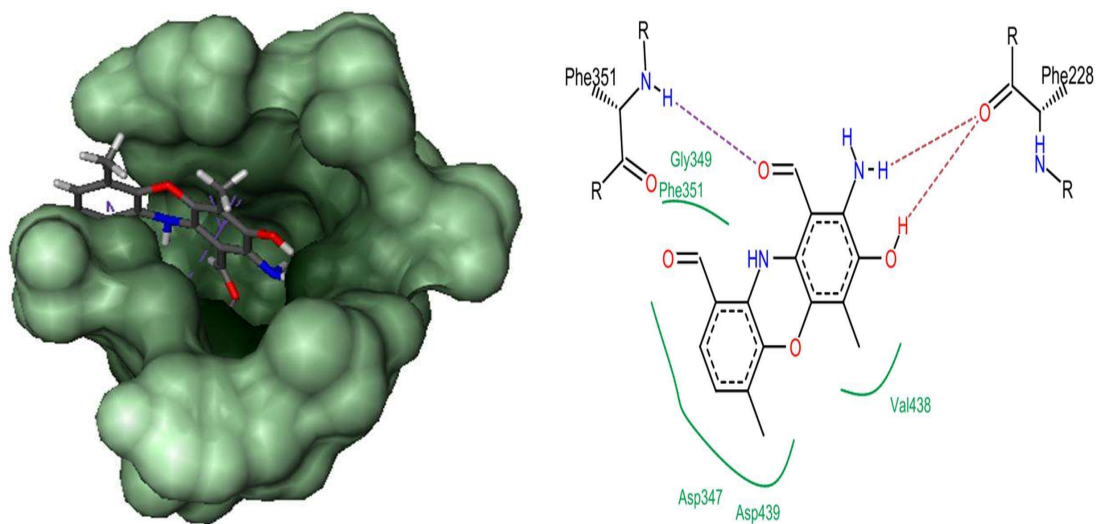
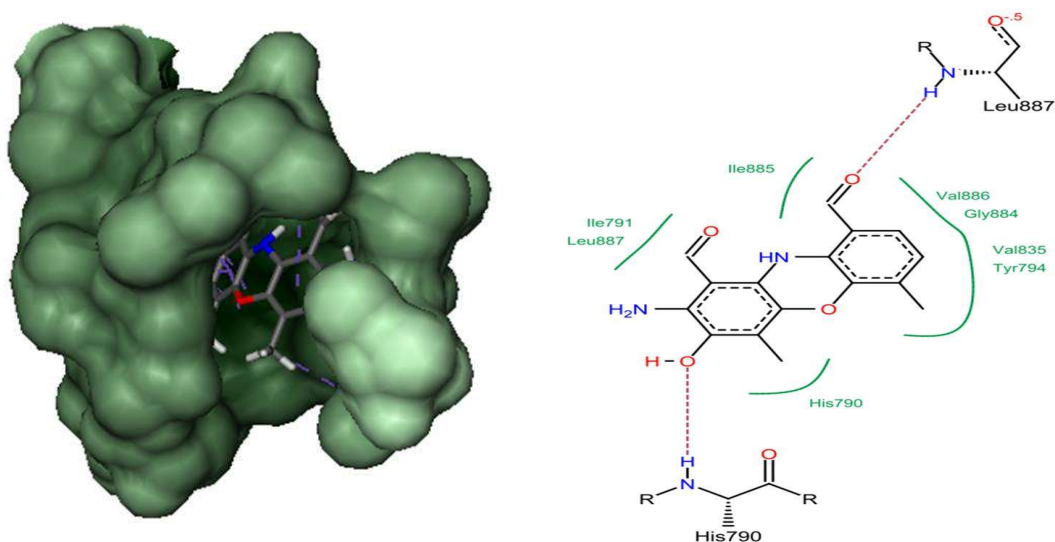


Figure 4. e. Docking complex and its interactions of rpoB from *Pseudomonas aeruginosa* and Actinomycin D. f. Docking complex and its interactions of rpoB from *staphylococcus aureus* and Actinomycin D





4. DISCUSSION

The target sequence and template structure are typically accurately aligned when there is a high amount of sequence identity. *Bacillus cereus*, *Escherichia coli*, *Enterobacter*, *Klebsiella pneumonia*, *Pseudomonas aeruginosa*, and *Staphylococcus aureus* had PDBIDs, sequence identities of their respective rpoBs of 66.46, 70.09, 100, 79.01, 99.54, and 98.88%, respectively, and fewer e-value were aligned. This result is consistent with the findings of Sekhar [21], who stated that sequences with the highest degree of identity and the lowest e-value were aligned and utilized as a reference structure to construct a three-dimensional (3D) model of rpoB. Using a protein's basic sequence and past knowledge gleaned through structural resemblances with other proteins, homology modeling is a technique for creating three-dimensional (3D) structures of proteins [22]. The objective of the current study was to establish the PDB ID structure as the homologous structure for the rpoB protein. Swiss Model Server was used to carry out the work using rpoB as a template for the prediction of 3D structure. Biomolecules like proteins are extremely flexible. From a functional standpoint, precise knowledge of protein structure is crucial. Using knowledge-based methods, protein structure prediction models the three-dimensional structure of a protein from its amino acid sequence [23].

Over 80% of the residues in the most favorable regions could be seen in the Ramachandran plot of all the rpoB models that had been generated. The model generated was found to be reliable and of good quality, according to the findings of ERRAT and Verify-3D, and made a comparable observation [24].

Tools like molecular docking have biomolecular simulated approaches built on integrated bioinformatic analyses that examine how molecules interact. They are frequently used as theoretical simulation techniques in drug development research [25]. The initially predicted binding site (in blue) is regarded as the ideal binding site and is employed in subsequent docking investigations.

The results of the docking interactions showed that *Staphylococcus aureus* rpoB and Actinomycin D interact strongly while *Pseudomonas aeruginosa* showed low interaction. The docking score ranges from -7.1652 kJ/mol to -9.2351 kJ/mol. Encounters while docking Actinomycin D are thought to interact with rpoB of *Escherichia coli*, *Bacillus cereus*, *Enterobacter*, and *Klebsiella pneumonia* through two bonded interactions and four non-bonded interactions. While it was found that eight amino acids were involved in the hydrophobic interactions in the case of *Staphylococcus aureus*, and only five amino acids were in *Pseudomonas aeruginosa*.

In *Bacillus cereus*, it has been found that the glutamine keto group (gln1072) favors the formation of an H-bond with the hydroxyl group and amino group of actinomycin D, while the lysine keto group (Lys 1098) favors the formation of an H-bond with the amide group of actinomycin D (Fig. 4.a). In *E. coli*, it seems to have been found that the phenylalanine keto group (Phe224) favours the formation of an H-bond with the hydroxyl group and amino group of actinomycin D, while the amino group from glycine (Gly 344) favors the formation of an H-bond with the keto group of actinomycin D. While in the cases of *Enterobacter* and *Klebsiella pneumonia*, the glycine (Gly344 and Gly355) and glutamic acid (Glu226 and Glu237) favour the H-bonds, respectively. Phenyl alanine's keto and amino groups (Phe 228 and Phe 351) in *Pseudomonas aeruginosa* favour the formation of an H-bond with Actinomycin D's hydroxyl and keto groups. *Staphylococcus aureus*'s amino groups Leucine (Leu887) and Histidine (His 790) encourage the formation of H-bonds with the hydroxyl and keto groups of the actinomycin D molecule.

Exploiting new molecular systems is important since infections are starting to become multi-drug resistant. Given the urgency of the situation, which even calls for the re-engineering and repositioning of some outdated drug families, the goal of this study is to fill a drug development pipeline with new drug revelation strategies that will incrementally improve upon existing structures.

5. CONCLUSION

An important and distinctively bacterial enzyme has long been a desirable therapeutic target and has steadfastly been pursued as a location for bactericide drug exploitation due to its critical nature and lack of a humanlike homolog. Actinomycin D significantly reduces both prokaryotic and eukaryotic cells' ability to synthesize DNA-dependent DNA and RNA. This research emphasizes the viability of creating unique compounds with small adjustments to the structure already present, and it aims to alter the process of developing medications. The creation of emerging therapies and interventions required to treat drug-resistant pathogens will be made possible by the use of bioinformatics tools, which also have the potential to enable a more logical and focused approach to the search for novel drug targets.

6. REFERENCES

- [1]. Vardanyan, R., & Hruby, V. (2016). *Synthesis of best-seller drugs*. Academic Press.
- [2]. Karol Angulo-Baltodano, Jimena Campos-Cubero, Sebastián Monge-Jiménez, Juan José Mora-Román, Rolando Vargas-Zúñiga, Daniela González-Corrales, & German Madrigal-Redondo. (2023). Use of microorganisms for biological and biotechnological drugs development. *International Journal of Modern Pharmaceutical Research*,7(4):01-04.

- [3]. Queiroz Sousa, M. D., Lopes, C. E., & Pereira Júnior, N. (2001). A chemically defined medium for production of actinomycin D by *Streptomyces parvulus*. *Brazilian Archives of Biology and Technology*,44(3):227-231.
- [4]. Rakhmawatie, M. D., Wibawa, T., Lisdiyanti, P., Pratiwi, W. R., & Damayanti, E. (2021). Potential secondary metabolite from Indonesian Actinobacteria (InaCC A758) against *Mycobacterium tuberculosis*. *Iranian Journal of Basic Medical Sciences*,24(8):1058-1068.
- [5]. Qureshi, K. A., Azam, F., Fatmi, M. Q., Imtiaz, M., Prajapati, D. K., Rai, P. K., Jaremko, M., Emwas, A., & Elhassan, G. O. (2023). *In vitro* and *in silico* evaluations of actinomycin X₂ and actinomycin D as potent anti-tuberculosis agents. *PeerJ*,11, e14502.
- [6]. Pancholi, A., Klingberg, T., Zhang, W., Prizak, R., Mamontova, I., Noa, A., Sobucki, M., Kobitski, A. Y., Nienhaus, G. U., Zaburdaev, V., & Hilbert, L. (2021). RNA polymerase II clusters form in line with surface condensation on regulatory chromatin. *Molecular Systems Biology*,17(9).
- [7]. Lai, W. S., Arvola, R. M., Goldstrohm, A. C., & Blackshear, P. J. (2019). Inhibiting transcription in cultured metazoan cells with actinomycin D to monitor mRNA turnover. *Methods*,155:77-87.
- [8]. Liu, X. F., Xiang, L., Zhou, Q., Carralot, J., Prunotto, M., Niederfellner, G., & Pastan, I. (2016). Actinomycin D enhances killing of cancer cells by immunotoxin RG7787 through activation of the extrinsic pathway of apoptosis. *Proceedings of the National Academy of Sciences*,113(38):10666-10671.
- [9]. Laszlo, J., Miller, D. S., McCarty, K. S., & Hochstein, P. (1966). Actinomycin D: Inhibition of respiration and glycolysis. *Science*, 151(3713):1007-1010.
- [10]. Holden, J. T., & Utech, N. M. (1967). Actinomycin D inhibition of amino acid transport in *Streptococcus faecalis*. *Biochimica et Biophysica Acta (BBA) - Biomembranes*,135(2):351-354.
- [11]. Baidara, P., & Mandal, S. M. (2020). Bacteria and bacterial anticancer agents as a promising alternative for cancer therapeutics. *Biochimie*,177:164-189.
- [12]. Mohan, C. D., Rangappa, S., Nayak, S. C., Jadimurthy, R., Wang, L., Sethi, G., Garg, M., & Rangappa, K. S. (2022). Bacteria as a treasure house of secondary metabolites with anticancer potential. *Seminars in Cancer Biology*,86:998-1013.
- [13]. Hafsa, U., Chuwdhury, G., Hasan, M. K., Ahsan, T., & Moni, M. A. (2022). An *in silico* approach towards identification of novel drug targets in *Klebsiella oxytoca*. *Informatics in Medicine Unlocked*,31:100998.
- [14]. Sreejisha, P. S., & Devika Pillai. (2014). Homology modelling of vp19 and its validation for prediction of novel binding sites for white spot syndrome virus. *Journal of Advanced Bioinformatics Applications and Research*,5(1).
- [15]. Parveen, A., Malashetty, V., Shetty, P., Patil, V., & Deshpande, R. (2022). Rapid and easy identification of genes associated with nanoparticles from plant protein structure database. *OpenNano*,8:100071.
- [16]. Jayabal, D., Jayanthi, S., & Gnanendra, S. (2020). Homology Modelling and Docking Studies of p85-alpha a subunit of Phosphatidylinositol 3-kinase with Anti-diabetic Compounds. *Journal of University of Shanghai for Science and Technology*,22(11):964-970.

- [17]. Elengoe, A. (2021). Computational approach in drug development for obesity. *Obesity and its Impact on Health*,167-181.
- [18]. Noor, H., Ikram, A., Rathinavel, T., Kumarasamy, S., Nasir Iqbal, M., & Bashir, Z. (2021). Immunomodulatory and anti-cytokine therapeutic potential of curcumin and its derivatives for treating COVID-19 – a computational modeling. *Journal of Biomolecular Structure and Dynamics*,40(13):5769-5784.
- [19]. Gohlke, H., Hendlich, M., & Klebe, G. (2000). Knowledge-based scoring function to predict protein-ligand interactions. *Journal of Molecular Biology*,295(2):337-356.
- [20]. Srinivasan, S., Sadasivam, S. K., Gunalan, S., Shanmugam, G., & Kothandan, G. (2019). Application of docking and active site analysis for enzyme linked biodegradation of textile dyes. *Environmental Pollution*,248:599-608.
- [21]. Sekhar, P. N., Amrutha, R. N., Sangam, S., Verma, D., & Kishor, P. K. (2007). Biochemical characterization, homology modeling and docking studies of ornithine δ -aminotransferase—an important enzyme in proline biosynthesis of plants. *Journal of Molecular Graphics and Modelling*,26(4):709-719.
- [22]. Hameduh, T., Haddad, Y., Adam, V., & Heger, Z. (2020). Homology modeling in the time of collective and artificial intelligence. *Computational and Structural Biotechnology Journal*,18:3494-3506.
- [23]. Agnihotry, S., Pathak, R. K., Singh, D. B., Tiwari, A., & Hussain, I. (2022). Protein structure prediction. In *Bioinformatics* pp.177-188.
- [24]. Mutheneni, S., & Josyula, J. N. (2021). In silico structural characterization of cytochrome C oxidase subunit 1: A transmembrane protein from *Aedes aegypti*. *Journal of Vector-Borne Diseases*,58(2):106.
- [25]. Vidal-Limon, A., Aguilar-Toalá, J. E., & Liceaga, A. M. (2022). Integration of molecular docking analysis and molecular dynamics simulations for studying food proteins and Bioactive peptides. *Journal of Agricultural and Food Chemistry*,70(4):934-943.